Biomaterials 31 (2010) 4517–4529

Contents lists available at ScienceDirect

Biomaterials

journal homepage: www.elsevier.com/locate/biomaterials

A functional extracellular matrix biomaterial derived from ovine forestomach

Stan Lun [a], Sharleen M. Irvine [a], Keryn D. Johnson [b], Neil J. Fisher [a], Evan W. Floden [a], Leonardo Negron [a], Sandi G. Dempsey [a], Rene J. McLaughlin [b], Madhusudan Vasudevamurthy [b], Brian R. Ward [a], Barnaby C.H. May [a,*]

[a] Mesynthes Limited, P.O. Box 31311, Lower Hutt 5040, New Zealand
[b] Industrial Research Limited, P.O. Box 31310, Lower Hutt 5040, New Zealand

ARTICLE INFO

Article history:
Received 13 January 2010
Accepted 10 February 2010
Available online 11 March 2010

Keywords:
ECM (extracellular matrix)
Wound healing
Tissue regeneration
Collagen
Fibroblast growth factor
Cell culture

ABSTRACT

Extracellular matrix (ECM) based biomaterials have an established place as medical devices for wound healing and tissue regeneration. In the search for biomaterials we have identified ovine forestomach matrix (OFM), a thick, large format ECM which is biochemically diverse and biologically functional. OFM was purified using an osmotic process that was shown to reduce the cellularity of the ECM and aid tissue delamination. OFM produced using this technique was shown to retain residual basement membrane components, as evidence by the presence of laminin and collagen IV. The collagenous microarchitecture of OFM retained many components of native ECM including fibronectin, glycosaminoglycans, elastin and fibroblast growth factor basic. OFM was non-toxic to mammalian cells and supported fibroblast and keratinocyte migration, differentiation and infiltration. OFM is a culturally acceptable alternative to current collagen-based biomaterials and has immediate clinical applications in wound healing and tissue regeneration.

1. Introduction

There is a move towards the clinical use of intact allogenic or xenogenic extracellular matrix (ECM) to facilitate tissue regeneration. These exogenous ECMs provide a native framework for cell adhesion at the site of a tissue deficit, therefore allowing local cells to migrate into the matrix, adhere and undergo differentiation [1]. Natural ECM-based biomaterials can remain intact at the site of implantation for 1–2 months [2], during which time the matrix is degraded by cellular proteases and new endogenous ECM is laid down by resident fibroblasts. Throughout this period of remodeling the exogenous ECM provides the necessary structural support and dynamically exchanges signals with local cells leading to tissue infill. ECM-based biomaterials stimulate rapid revascularization of tissue relative to synthetic and semi-synthetic matrices [3]. This effect is thought to be due to the presence of stimulatory factors and adhesion molecules that promote the proliferation of endothelial cells within remnants of native vascular channels [4]. These biomaterials are relatively immunologically inert [5], and resistant to adhesions [6] and encapsulation [7]. Infection rates of ECM-based biomaterials are relatively low [8], a feature that may be attributable to their inherent antimicrobial activity [9], and/or their ability to rapidly vascularize and therefore clear bacteria. As well as their reported bioactivity and bioinductive effects [1], the biophysical properties of ECM-based biomaterials can be engineered to make these materials suitable for load-bearing applications where they can provide structural integrity during the remodeling process [10].

Several commercial ECM-based biomaterials have become widely available for clinical use [11], and their adoption into practice has been leveraged off positive clinical evidence. Clinical applications have included hernioplasty, breast reconstruction, chronic wound healing, and the repair of rotator cuffs, urological defects, and dura mater [1]. Processes that decellularized native ECM to generate ECM-based biomaterials have been applied to a number of different tissue sources [11]. Being derived from native ECM, these biomaterials are primarily composed of collagens (types I and III), but can also include additional ECM-associated components, for example, elastin, laminin, fibronectin, glycosaminoglycans, growth factors and bioactive peptides [11]. The presence of additional minor components is dependent on the source of the raw material, and importantly the method of processing used during purification of the ECM [12]. Manufacturing can also alter the microarchitecture of the ECM by denaturing structural proteins [13].

As part of an effort to identify functional biomaterials for tissue regeneration we have developed a decellularized ECM from ovine forestomach tissue. Given its relative size, and the thickness of ECM

* Corresponding author.
E-mail address: barnaby.may@mesynthes.com (B.C.H. May).

0142-9612/$ – see front matter © 2010 Elsevier Ltd. All rights reserved.
doi:10.1016/j.biomaterials.2010.02.025

in this organ, forestomach tissue offers a solution to generate relatively large format ECM-based biomaterial with good performance characteristics. Additionally, ovine tissue was selected as it was thought that these presented a low barrier to clinical acceptance on cultural and religious grounds, as well as presenting a low risk with respect to viral pathogens and prions. The ovine forestomach matrix (OFM) was produced using a method of decellularization, termed 'sealed transmural osmotic flow' (STOF), whereby an osmotic gradient was used to draw detergent solutions across tissues, leading to decellularization and aiding delamination of the tissue layers. The structural features of OFM, in combination with the native and bioactive secondary macromolecules, provide a functional biomaterial for wound healing and tissue regeneration applications.

2. Materials and methods

2.1. General

All incubations were conducted at room temperature unless otherwise stated. Absorbance was recorded using an Opsys MR™ (Dynex Technologies – Virginia, USA) plate reader. All tissues were powdered with the aid of liquid nitrogen and a spice grinder prior to extraction and biochemical analysis. All biochemical analyses were expressed as concentration based on the starting weight of powdered tissue. In the absence of ovine specific antibodies appropriate alternatives were used and their cross-reactivity with ovine antigens confirmed. Porcine small intestinal submucosa (SIS, OaSIS®) was obtained from Cook Biotech (Healthpoint Limited – Texas, USA). Light microscopy was conducted using an Olympus IX71 microscope and fluorescence microscopy using an Olympus BX51 microscope (ex 320–370/em 400 nm). Images were captured using a DP20 camera (Olympus – Japan) and AnalySIS software. Human D551 fibroblasts (CCL-110, ATCC) were cultured in Dulbecco's Minimal Essential Media (DMEM) supplemented with 10% fetal calf serum (FCS, Invitrogen – California, USA) (DMEM10). Pheochromocytoma cells (PC12) were grown in DMEM10 supplemented with 5% horse serum (Invitrogen). Human keratinocytes (CCD-1106 ATCC) were maintained in Epilife® (Invitrogen) supplemented with 1% Human Keratinocyte Growth Supplement (Invitrogen). All media contained 100 U/mL penicillin (Invitrogen), 100 μg/mL streptomycin (Invitrogen) and 1.25 μg/mL amphotericin B (Invitrogen), and all cultures were incubated at 37 °C containing 5% CO_2. D551 and keratinocytes were split using 0.25% trypsin (Invitrogen) at 37 °C for 5 min. PC12 cells were split by gentle repeated aspiration.

2.2. Decellularization of ovine forestomach using sealed transmural osmotic flow (STOF)

Intact ovine forestomachs were collected from New Zealand sheep, less than 18 months old (Taylor Prestons Limited – Wellington, New Zealand), and stored at 4 °C prior to use. In this instance, we referred to the forestomach as containing the rumen only, as tissues from the reticulum, omasum and abomasum were discarded. Animals were slaughtered according to New Zealand Food Safety Authority requirements, in accordance with the United States Department of Agriculture guidelines. OFM was produced using a proprietary process, termed 'sealed transmural osmotic flow', that employed an osmotic gradient and aqueous detergent solutions to facilitate removal of the epithelial and muscle layers, and decellularization of forestomach tissue [14]. The resultant OFM was chemically disinfected according to established procedures [15], lyophilized and terminally sterilized using ethylene oxide.

2.3. Histology

Formalin-fixed (5% formalin in PBS) tissues were placed in a cassette and processed for 12 h in a TissueTek™ VIP Tissue Processor (Sakura – California, USA). Cassetted tissues were orientated into paraffin blocks and cooled prior to microtomy (HM325, Microm – Germany). Blocks were 'rough cut' to expose tissue, placed onto ice then sections cut at 5–10 μm and floated onto poly-lysine slides (Superfrost R Plus, Menzel-Glaser – Germany). Slides were left to dry prior to staining. Sections were stained using hematoxylin and eosin [16], whereby the nuclei of the cells were stained with Gills hematoxylin, followed by a counter stain with 1% ethanolic eosin. Collagens I and III were stained on tissue sections using the method of Herovici [17]. The relative abundance of collagens I (red) and III (blue) in Herovici stained slides was quantified using ImageJ (National Institute of Health – Maryland, USA). Tissues were stained for glycosaminoglycans according to a modified Safranin-O and Fast Green staining method [18]. All slides were cover-slipped with Eukitt™ Mounting Media (Electron Microscopy Sciences – Pennsylvania, USA).

2.4. Tissue staining for DNA

Tissues were formalin fixed, mounted and sectioned, as described above. Slides were deparaffinized (100% xylol, 3 × 5 min washes), then rehydrated (100% ethanol, 70% ethanol, then PBS). Hoechst dye (Sigma – Missouri, USA) was added onto the slides (100–200 μL per slide) as a 1 μg/mL solution in 0.1% BSA/PBS, and incubated for approximately 1–2 min. The slide was washed in PBS, then incubated in PBS overnight in the dark. Slides were imaged and fluorescence quantified using ImageJ.

2.5. Immunohistochemical staining for laminin and collagen IV

Tissue sections were prepared as described above. Sections were washed in 100% xylol (3 × 5 min), then rehydrated by incubating in descending concentrations of alcohol (100%, 70%, 30% ethanol in water) for at least 5 min each. Sections are then placed in PBS for 5 min to fully rehydrate, and then endogenous peroxidases were quenched using 1% H_2O_2 in 70% methanol for 20 min. Sections were washed (3 × 5 min) in PBS then blocked (DAB Secondary Detection Kit, Millipore) for 30 min in a humidified chamber. Sections were rinsed under running water, then probed either with rabbit anti-human collagen IV primary antibody (1:1000 dilution, Abcam – Massachusetts, USA) or rabbit anti-human laminin (1:1000 dilution, Abcam), both diluted in 1% BSA/PBS. Sections were incubated for 30 min in a humidified chamber then washed (3 × 5 min) in 0.1% Triton X-100/PBS, then PBS (5 min). Sections were developed using a DAB Secondary Detection Kit (Millipore – Massachusetts, USA), according to the manufacturer's instructions, and counterstained with Harris' hematoxylin solution, diluted to 10% in water. Sections were dehydrated through graded ethanol, cleared in xylol and air dried overnight prior to mounting with DPX mountant.

2.6. Scanning electron microscopy

Sections of tissue measuring approximately 3 × 3 mm were mounted onto an SEM platform using carbon adhesive tape and carbon coated using an Emitech CC7650 carbon coater (Quorum Technologies – UK) for 10 s at a pressure of 0.2 mTorr. The carbon coated sample was imaged using a Leo 440 SEM (Leo – UK), fitted with an Oxford EDS system (Oxford Instruments – UK). Images were recorded using Link ISIS software (Oxford Instruments). Fiber thicknesses were measured using ImageJ.

2.7. Quantification of total collagen

Total collagen was quantified using a hydroxyproline analysis of acid hydrolyzed tissues [19]. Briefly, powdered tissues (approx. 50 mg) were heated at 120 °C for 60 min in 6 M HCl (500 μL). Samples were allowed to cool, and then evaporated with the aid of a vacuum centrifuge. The pellet was rinsed with RO H_2O (100 μL), then the samples again dried under vacuum. Neutralization buffer (0.16 M citric acid, 0.59 M sodium acetate, 0.56 M sodium hydroxide, 0.8% glacial acetic acid, 20% isopropanol in water) (500 μL) was added to each sample, along with a freshly prepared solution of chloramine-T (0.05 M, 100 μL). Samples were incubated for 20 min with shaking. Erlich's solution (100 μL, 1 M *p*-dimethylaminobenzaldehyde, 60% isopropanol, 26% perchloric acid in water) was added, and the samples heated at 65 °C for 45 min. Samples were cooled, then 200 μL transferred to a 96 well plate (Jet Biofil, – Guangzhou, China). Absorbance at 550 nm was measured and concentration of the solutions calculated from a standard curve of hydroxyproline (Sigma). Total collagen was calculated assuming a mass ratio of hydroxyproline:total collagen of 7.14:1 [20].

2.8. SDS-PAGE collagen analysis

Weighed samples of OFM (approx. 50 mg) were incubated for 16 h with 5 mg pepsin (450 U/mg, Sigma), as a 5 mg/mL solution in aqueous 0.5 M acetic acid. Samples of ovine forestomach were similarly digested using pepsin (5 mg/mL) at 4 °C for 2 h. Samples were centrifuged at 12k rpm for 10 min and the supernatant collected. Forestomach tissue extracts were further purified using a salt precipitation (2 M NaCl, 4 °C, 18 h). The salt precipitated pellet was resuspended in tris-acetate buffer containing 2 M urea and 2.6% SDS (pH 8.1). Protein concentration of the samples was normalized to approximately 1 mg/mL following BCA protein determination. All samples were loaded on a NuPAGE® Novex tris-acetate gel (Invitrogen) composed of a 3–8% (w/v) running gel and run at 150 V using a tris-acetate running buffer (Invitrogen). Samples run under delayed reducing were prepared in Laemmli loading buffer containing 1% SDS, 10% glycerol and 0.004% bromophenol blue and incubated at 60 °C for 30 min [21]. Samples were additionally prepared in Laemmli loading buffer containing 3% β-mercaptoethanol and incubated at 100 °C for 15 min prior to loading on the gel. Pre-stained molecular weight standards (Sigma), as well as, purified human placenta collagen I and human placenta collagen III (Sigma) were included. Following electrophoresis, gels were stained using Coomassie Brilliant Blue G 250 (Bio-Rad) and imaged using a MultiImage system (Alpha Innotech Corporation – California, USA) and the densitometry of protein bands α1(I), α2(I), α(III) quantified using ImageJ (NIH). The proportion of collagen III was determined from the densitometric units using the following: $\alpha1(III)/\alpha1(I) + \alpha2(I) + \alpha(III)$.

2.9. Quantification of collagens I, III and IV by ELISA

Weighed samples of OFM and ovine forestomach were pepsin digested as described above. Collagens I, III and IV were quantified in pepsin extracts using separate indirect ELISA methods. A pepsin-digested extract (50 μL) was transferred to a 96-well microtiter plate (NUNC – New York, USA) and incubated with 100 mM carbonate coating buffer (pH 9.6) for 2 h, or overnight at 4 °C. The plate was washed with TBST (20 mM Tris, 137 mM NaCl, 0.05% Tween 20, pH 7.5), then blocked with 1% BSA/PBS (250 μL/well) for 1 h. The plate was again washed and to each well was added 100 μL of rabbit antibodies against collagen I, collagen III, or collagen IV (Abcam). In all cases, the appropriate antibody was diluted 1/5000 in 0.1% BSA, and the plate incubated for 2 h. The plate was washed, then 100 μL of goat anti-rabbit antibody-HRP conjugate (1/10,000 in 1% BSA) (Abcam) was added and the plate incubated for 2 h. The plate was washed, and then 100 μL of TMB solution (Sigma) was added. Development of the plate was stopped with aqueous 1 M HCl stop reagent, after approximately 10 min. Absorbance (450 nm) was quantified, and concentration of the pepsin-digested extracts calculated from a standard curve of either rat tail collagen I (Gibco – California, USA), human collagen III (Millipore) or bovine collagen IV (Millipore). The collagen cross-reactivity of each of the antibodies was confirmed to be less than 15% using purified standards of collagens I, III and IV.

2.10. Lipid and elastin quantification by mass balance

Powdered tissue (approx. 50 mg) was heated at 37 °C for 60 min, cooled and reweighed until a stable dry weight had been achieved. The sample was extracted with ethanol/diethyl ether (1:1, 1 mL) for 15 min, and then centrifuged at 13k rpm for 10 min. The supernatant was discarded and the pellet again extracted with ethanol/diethyl ether. Ethanol/diethyl ether extraction was repeated three times, then the sample dried at 37 °C for 1 h, or until a constant weight had been achieved. Lipid content was reported as the mass difference before and after ethanol/diethyl ether extraction. The pellet was resuspended in a 0.3% SDS solution in water (1 mL) and incubated overnight with shaking. The suspension was centrifuged at 13k for 10 min and the supernatant discarded. The remaining pellet was resuspended in 0.3% SDS (0.5 mL) and incubated for 15 min with shaking. The sample was centrifuged (13k rpm, 10 min) and the supernatant discarded. The pellet was resuspended in aqueous 0.1 M NaOH solution (500 μL) and heated at 100 °C for 15 min. The suspension was centrifuged (13k rpm, 10 min), and the supernatant discarded. The remaining pellet was extracted with 0.1 M NaOH solution and centrifuged three more times. The pellet was dried to constant weight at 65 °C. The total elastin content was determined from the mass difference of the sample before SDS extraction and after NaOH extraction, and expressed as a concentration of starting powdered tissue.

2.11. Papain digestion

Powdered tissue (approx. 50 mg) was digested with 1 mg/mL papain (Sigma) solution in digestion buffer (1 M NaCl, 5 mM cysteine HCl, 1 mM EDTA in PBS pH 7.4) at 65 °C for 16 h. The sample was centrifuged (13k rpm, 20 min) and the pellet discarded. Sodium chloride (solid) was added to the supernatant to give a 4% solution. Four equal volumes of ethanol were added and the solution incubated at −20 °C for 2 h. The sample was centrifuged (4k rpm, 20 min) and the supernatant discarded. The precipitated GAG fraction was resuspended in water (1 mL) prior to analysis.

2.12. Quantification of total GAGs and heparan sulfate

Samples were quantified using a Blyscan™ Sulfated Glycosaminoglycan Assay Kit (Biocolor) using modifications to the manufacturer's instructions. Prior to analysis samples were either digested with heparin lyase or undigested. Digested samples were treated with 0.5 mU heparin lyases I, II and III (Seikagaku Corporation – Japan) and incubated at 37 °C for 24 h. Blyscan™ dye solution (750 μL) was added to lyase-digested or undigested samples (100 μL), and incubated for 30 min with shaking. Samples were centrifuged (12k rpm, 10 min) and the supernatant carefully discarded. The pellet was fully solubilized in dye dissociation buffer (750 μL) with the aid of a vortex mixer. Samples (200 μL) were transferred to a clear bottom microtiter plate and absorbance quantified at 656 nm. The concentration of GAGs was quantified from a standard curve of chondroitin sulfate. Heparan sulfate was calculated from the difference between lyase treated and untreated samples.

2.13. Quantification of hyaluronic acid

Extracts were analyzed for HA using a Hyaluronan HA-ELISA Kit (Echelon Biosciences Inc. – Utah, USA), according to the manufacturer's instructions. Briefly, 150 μL aliquots of papain-digested samples were added to 75 μL 'Working Detector' solution and the mixture incubated at 37 °C for 60 min. The solution (100 μL) was transferred to a prepared ELISA plate and incubated on the plate for 60 min at 37 °C. The plate was subsequently washed with TBST (20 mM Tris, 137 mM NaCl, 0.05% Tween 20, pH 7.5), then 100 μL of 'Working Substrate' solution was added to each well. The plate was incubated for 45 min, quenched with 'Stop' solution and the plate read at 405 nm. The concentration of HA in the extract was determined from a standard curve of purified HA (Echelon).

2.14. Quantification of DNA

A papain-digested supernatant (100 μL) was transferred to a microtiter plate and Hoechst 33258 (Sigma) dye (100 μL) was added, as an aqueous 0.1 μg/mL solution, and the mixture incubated for 5 min. The fluorescence intensity of the samples was measured using a Fluoroskan® Ascent (Thermo Scientific – Massachusetts, USA). The concentration of DNA was calculated from a standard curve of calf thymus DNA (Sigma) and expressed relative to the starting weight of tissue.

2.15. Quantification of fibroblast growth factor basic

Powdered tissues (approx. 50 mg) were extracted with SDS extraction buffer (4% SDS, 0.02 M Tris buffer, pH 8.0, 65 mM dithiothreitol, 2 mM EDTA, 2 mM PMSF, 2 mM *N*-ethylmaleimide) for 16 h at 37 °C. Samples were centrifuged at 12k rpm for 10 min and the supernatant carefully removed. The extract was dialyzed (3.5 kDa) against PBS (5 L) for 24 h at 4 °C. The extract was analyzed using a Human FGF-basic ELISA Development Kit (Peprotech – New Jersey, USA). The capture antibody rabbit anti-human FGF2 was diluted to 2 μg/mL with PBS, and 100 μL transferred to a 96-well ELISA plate (NUNC). The plate was coated with capture antibody overnight with gentle mixing. The plate was washed five times with TBST, then blocked with 1% BSA/PBS (300 μL/well), for 1 h. The blocking solution was removed and the plate washed three times with TBST. Samples (100 μL) were transferred to the plate and incubated for 2 h with shaking, then the plate was washed five times with TBST. The plate was emptied and detection antibody biotinylated rabbit anti-human FGF2 (100 μL) was added as a 1 μg/mL solution in 0.1% BSA/PBS. The plate was incubated for 2 h then washed five times with TBST. Avidin-HRP conjugate (100 μL), previously diluted 1/200,000 in 1% BSA/PBS, was added and the plate incubated for 30 min. The plate was washed with TBST, then developed with 100 μL TMB solution (Sigma). Development was stopped by the addition of 1 M HCl (100 μL) and absorbance at 450 nm measured. Concentration of FGF2 was calculated from a solution of human recFGF2 (Peprotech).

2.16. Quantification of fibronectin

Powdered tissues (approx. 50 mg) were extracted with SDS extraction buffer (4% SDS, 0.02 M Tris buffer, pH 8.0, 65 mM dithiothreitol, 2 mM EDTA, 2 mM PMSF, 2 mM *N*-ethylmaleimide) for 16 h at 37 °C. Samples were centrifuged at 12k rpm for 10 min and the supernatant carefully removed. The extract was dialyzed (3.5 kDa) against PBS (5 L) for 24 h at 4 °C. The extract was analyzed using a QuantiMatrix™ Human Fibronectin ELISA Kit (Millipore), according to the manufacturer's instructions. Dialyzed solutions (110 μL) were premixed with rabbit anti-human fibronectin antibody (110 μL) and incubated for 30 min. A precoated ELISA plate was rehydrated with wash buffer for 15 min prior to samples being transferred to the plate (100 μL). The plate was incubated for 2 h, then washed five times with wash buffer. Goat anti-rabbit-HRP conjugate, previously diluted 1/10,000 in 1% BSA/PBS, was added to each well (100 μL) and the plate incubated for 60 min. The plate was washed five times, then developed with TMB solution (Sigma). Development was stopped by the addition of aqueous 1 M HCl solution and the absorbance at 450 nm measured. Fibronectin concentrations were calculated from a standard curve of purified human fibronectin.

2.17. Quantification of laminin

Powdered tissues (approx. 50 mg) were extracted with SDS extraction buffer (4% SDS, 0.02 M Tris buffer, pH 8.0, 65 mM dithiothreitol, 2 mM EDTA, 2 mM PMSF, 2 mM *N*-ethylmaleimide) for 16 h at 37 °C. Samples were centrifuged at 12k rpm for 10 min and the supernatant carefully removed. The extract was dialyzed (3.5 kDa) against PBS (5 L) for 24 h at 4 °C. The extract was analyzed according to the manufacturer's instructions using a QuantiMatrix™ Human Laminin ELISA Kit (Millipore). Briefly, samples were preincubated with rabbit anti-human laminin antibody for 10 min. The sample/antibody mixtures (100 μL) were transferred to a precoated ELISA plate, previously rehydrated in wash buffer (200 μL) for 15 min. The plate was incubated for 1 h, and then washed five times with wash buffer. Goat anti-rabbit-HRP conjugate (100 μL), diluted 1/10,000 in 1% BSA/PBS was added and the plate incubated for 30 min. The plate was washed five times with wash buffer, and then TMB solution (100 μL) was added to each well. Development of the plate was stopped by the addition of 1 M HCl (100 μL), and the plate read at 450 nm. Laminin concentrations of the samples were extrapolated from a standard curve of human laminin (Millipore).

2.18. MEM elution assay

Lyophilized OFM sheets were incubated at 37 °C for 24 h in DMEM, at a ratio of 64 cm^2 OFM per 10.6 mL DMEM. OFM was removed and the media was 0.2 μm sterile filtered and then FCS added to give a final concentration of 10%. Detroit 551 normal human fibroblasts (D551) were plated to 24-well plates at 70,000 cells/well

containing 1 mL DMEM10 and incubated for 24 h until 80% confluent. Media was carefully aspirated from a cell monolayer and replaced with the OFM-conditioned media (1 mL). Cells were incubated for three days at which time cell viability was quantified using the MTT assay, according to established procedures [22].

2.19. Cell adhesion assay

Discs of OFM (16 mm) were created using a sterile biopsy punch, and incubated at 37 °C for 24 h in DMEM10 (approx. 2 mL). OFM discs were removed from media and transferred to 24-well plates. Discs were secured to the bottom of the plates with the aid of a stainless steel ring (internal diameter 7 mm), with either the luminal or abluminal surface of the discs facing upwards. D551 or normal human keratinocytes were grown to approximately 80% confluency, and then split to 200k cells/mL in the appropriate culture media. Cells (1 mL) were transferred onto the surface of the OFM discs via the middle of the stainless steel ring. In this way, cells were unable to migrate around the edge of the disc and contaminate the underside. Cultures were incubated for 3 h, at which time OFM discs were removed, gently agitated to remove unbound cells, and transferred to 10% formalin in PBS. Discs were sectioned, deparaffinized and rehydrated, as described above, then mounted in the dark with ProLong Gold Mounting Media with DAPI (Invitrogen). Attached cells were visualized using a fluorescent microscope and the total number of cells present on the each section counted manually. Statistical analysis of cell adhesion was conducted using an unpaired *T*-Test (Prism, GraphPad – California, USA).

2.20. Cell infiltration assay

OFM discs (16 mm) were rehydrated as described above. Discs were transferred to 24-well plates, and held in place with stainless steel rings with the abluminal surface facing upwards. D551 cells at approximately 80% confluency were split and resuspended in DMEM10 at 50k cells/mL. D551 cells were transferred to the discs and the cultures incubated for up to 10 days with media changes every 48 h. Discs were removed from culture at 12 h, and days 1, 2, 3, 5, 8 and 10, gently agitated to remove unbound cells, then fixed, sectioned, mounted and DAPI stained, as described above. Sections were visualized using fluorescence microscopy.

2.21. PC12 cell differentiation assay

PC12 cells were seeded at 4000 cells per well on 96-well plates containing 200 μL DMEM. Cells were incubated until attached (approx. 30 h). Extracts of powdered OFM were prepared using 4% SDS extraction buffer (4% SDS, 0.02 M Tris buffer, pH 8.0, 65 mM dithiothreitol, 2 mM EDTA, 2 mM PMSF, 2 mM *N*-ethylmaleimide, 37 °C, 24 h). The extract was centrifuged and the supernatant dialyzed against PBS for 24 h. The protein concentration of the SDS extract was determined using the BCA protein assay (Pierce), according to the manufacturer's instructions. Where necessary, FGF2 was neutralized by incubating the SDS extracts at 37 °C for 30 min with rabbit anti-human FGF2 antibody (Peprotech) diluted 1:50, 1:100 and 1:200. All SDS extracts were diluted 1:10 in DMEM, filter sterilized (0.2 μm), then transferred (200 μL) to the PC12 monolayer. Extracts were additionally prepared by incubating powdered OFM in DMEM (37 °C, 24 h). The suspension was centrifuged (13k rpm, 10 min) and the supernatant collected and filter sterilized (0.2 μm). Media was aspirated from the PC12 monolayer, and replaced with 200 μL of extract. In all experiments, cells treated with human recFGF2 (50 ng/mL final concentration, Peprotech), and untreated cells, served as positive and negative controls, respectively. Cells were incubated for 48 h. The cell monolayer was imaged using two frames per well, and the cells and cell processes manually counted from examination of the digital images. Neuronal processes were defined as outgrowths whose length extended at least the width of one cell body. Cell differentiation was expressed as the average number of cell processes per cell.

3. Results

3.1. STOF processing of forestomach tissue

While the forestomach of ruminants is composed of the reticulum, rumen, omasum and abomasum, we extracted ECM from the rumen only and referred to the rumen as the 'forestomach'. Forestomach tissue comprises three distinct tissue layers, the tunica muscularis, propria submucosa and lamina epithelias. Only the ECM contained within the propria submucosa of the rumen was isolated to yield OFM, therefore requiring that the three tissue layers be separated. Sealed transmural osmotic flow (STOF) was used to aid delamination of the three tissue layers, as well as, decellularize the propria submucosa ECM. In this instance, hypotonic solutions of either a non-ionic or a cationic detergent were used in conjunction with hypertonic aqueous NaCl solutions during the STOF process. By using the forestomach tissue to separate the hypotonic detergent solutions and hypertonic salt solutions, an osmotic gradient was established which had the effect of drawing detergents into and through the forestomach tissue. It was found that the orientation of the tissue relative to the osmotic gradient was critical to the effectiveness of the STOF process. STOF treatment of forestomachs in their natural orientation (i.e. epithelial layer on the interior, muscle layer on the exterior), yielded tissue that was grossly denatured and therefore difficult to delaminate. In contrast, when the intact forestomach was everted, such that the epithelial layer was on the exterior and the muscle layer on the interior, forestomachs could easily be delaminated with scraping or mechanical delamination. Tissue orientation with respect to the osmotic gradient was therefore critical in determining effective delamination. Delamination of the tissues was evidenced by H&E staining of the OFM following STOF treatment (Fig. 1A and B). Both the tunica muscularis and lamina epithelias' layers of the forestomach tissue were removed, leaving the propria submucosa intact. The propria submucosa contained an especially dense layer of collagenous matrix that extended into the remnants of the forestomach papillae (indicated by ⇐ in Fig. 1B). Papillae lengths and thicknesses ranged from 165 to 656 μm and 42 to 162 μm, respectively and as such, were approximately double the size of human dermis rete ridges [23,24].

The critical features in the production of ECMs for clinical applications are steps to reduce the cellularity of the collagen matrix and therefore reduce any negative host response to the xenoplant. We used the presence of nucleic acids as a surrogate marker for the cellularity of OFM. The extent of decellularization of OFM was qualified using Hoechst staining of OFM sections, as well as, quantification of total DNA in papain-digested extracts. Hoechst 33258 stained OFM sections (Fig. 1D) demonstrated greatly reduced nucleic acid staining relative to raw tissue sections (Fig. 1C). Quantification of punctate nuclear staining in tissue sections demonstrated a reduction of approximately 80% in the cellularity of OFM, relative to the ovine forestomach (data not shown). Total DNA was additionally quantified in papain-digested OFM and ovine forestomach tissues using a fluorescent dye-binding assay. The concentrations of DNA in OFM and ovine forestomach were 1.7 ± 0.5 mg/g and 9.0 ± 0.5 mg/g, respectively (Table 1A), which represented an approximately 80% reduction in DNA concentration following STOF tissue decellularization. We extended this study to understand the DNA concentration of a commercially available ECM biomaterial, namely small intestinal submucosa (SIS or OaSIS®). In our hands, the DNA concentration of SIS (2.7 ± 0.2 mg/g) was greater than previously reported [25], and both OFM and SIS had equivalent DNA concentrations.

3.2. Characterization of the basement membrane components

The basement membrane is a specialized form of ECM that represents a contiguous layer of cells and fibers that underlies the epithelial layer and anchors it to deeper connective tissues. OFM tissue sections were probed using either an anti-collagen IV or anti-laminin antibody to probe the existence of basement membrane components. Immunohistochemistry revealed that both collagen IV and laminin were colocalized to the luminal surface of OFM, as seen in ovine forestomach (Fig. 2, indicated by ←). Basement membrane components were also evidenced in the lamina epithelias removed during the STOF process (Fig. 2). That collagens IV and laminin were detected in the lamina epithelias is evidence that the basement membrane seen in OFM is not intact as seen in forestomach tissue. Instead, residual components of the basement membrane remain in OFM after fracturing of the basement membrane to facilitate

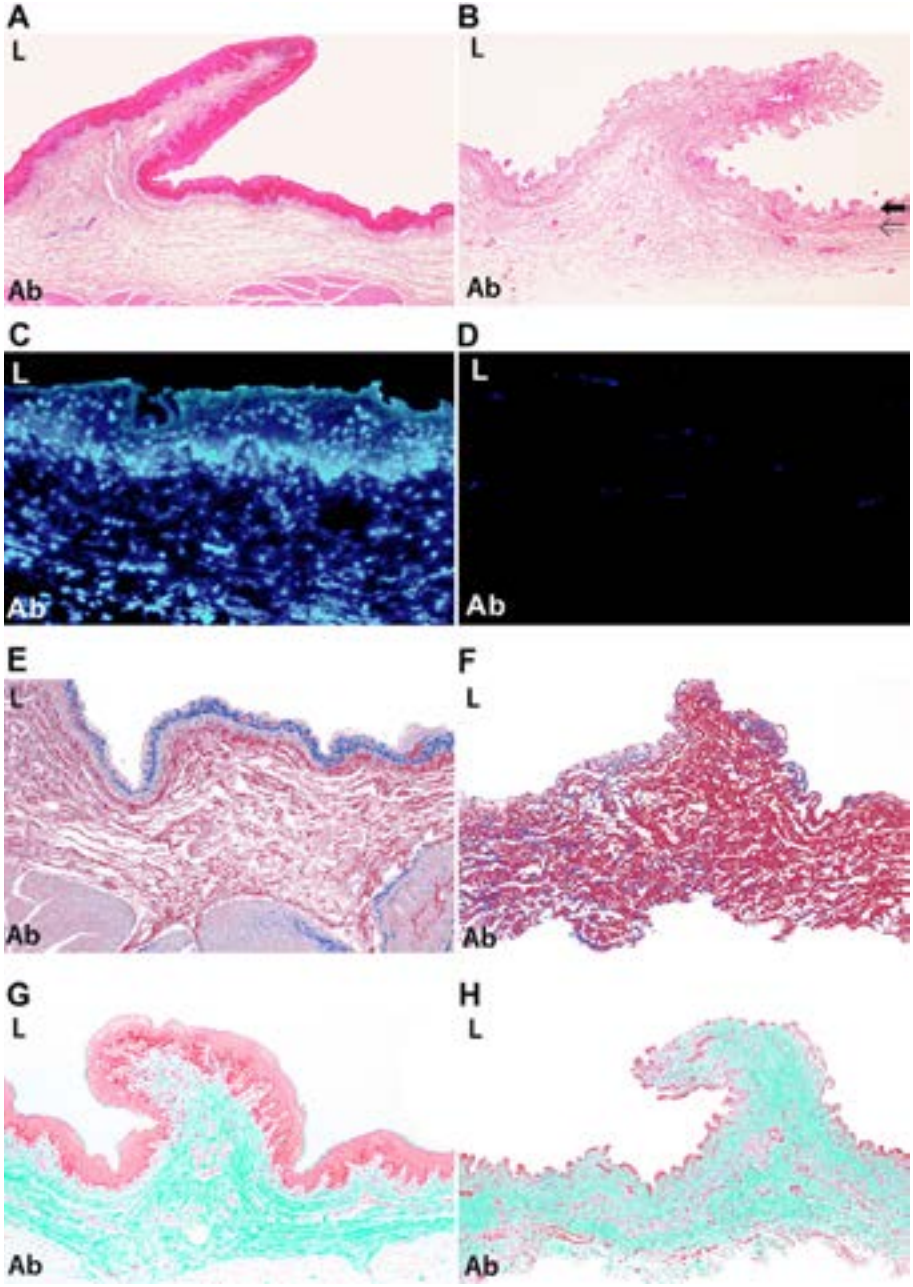

Fig. 1. H&E staining of the ovine forestomach (A) and OFM (B). Location of the residual basement membrane components '←', and dense connective layer '⇐'. 4× Magnification. Representative images of Hoechst 33258 stained sections of forestomach tissue (C) and OFM (D). Cells appear as intense blue fluorescence while the matrix and connective tissues appear more diffuse. 20× Magnification. Herovici staining of collagen I (red) and collagen III (blue) in forestomach tissue (E) and OFM (F). 4× Magnification. Safranin-O/Fast green staining of proteoglycans (red) in forestomach tissue (G) and OFM (H). 4× Magnification. Luminal and abluminal surfaces are indicated with 'L' and 'Ab', respectively.

removal of the lamina epithelias. Dense collagen IV and laminin staining was also evident in the remnants of blood vessels, consistent with a sub-endothelial basement membrane (Fig. 2, inserts). Collagen IV additionally localized to the dense collagen layer underlying the basement membrane and previously noted by H&E staining (Fig. 2B, indicated by ⇐).

3.3. The microarchitecture of OFM

OFM was prepared and lyophilized sections were imaged using scanning electron microscopy (SEM) (Fig. 3). The OFM was clearly anisotropic with differences in the luminal and abluminal surface contours seen by SEM (Fig. 3A). The luminal face, resulting from removal of the epithelial layer, had a smooth continuous surface that was thought to arise from remnants of the basement membrane (Fig. 3C) [26]. In contrast, the abluminal face contained surface striations, most likely due to the open reticular structure, as seen by histology (Fig. 3D). Within the OFM a detailed collagen microarchitecture was evident containing numerous interlacing fibers of various thicknesses, pores and open channels (Fig. 3B). There was no evidence of denaturation of the collagen framework. Matrix fiber thicknesses were measured from SEM images using ImageJ and ranged from 0.8 to 11.6 μm, with an average thickness of 4.1 ± 0.1 μm. This is consistent with previously reported collagen fiber thicknesses [27].

Table 1A
Major biochemical components of the ovine forestomach and OFM.

	Ovine forestomach (mg/g ± SE)	OFM (mg/g ± SE)
Total collagen	142.7 ± 9.7	821.0 ± 9.0
Collagen I	81.2 ± 6.6	738.8 ± 63.3
Collagen III	61.3 ± 0.7	196.8 ± 6.9
Collagen IV	5.4 ± 1.1	9.7 ± 2.1
Elastin	30.9 ± 6.4	27.5 ± 4.5
Total GAGs	3.9 ± 0.1	0.74 ± 0.01
Heparan sulfate	N.D.	0.31 ± 0.01
Hyaluronic acid	1.95 ± 0.02	0.4 ± 0.1
DNA	9.0 ± 0.5	1.7 ± 0.5
Lipid	50.2 ± 2.9	59.0 ± 5.2

Table 1B
Minor biochemical components of the ovine forestomach and OFM.

	Ovine forestomach (μg/g ± SE)	OFM (μg/g ± SE)
Fibronectin	15.30 ± 1.17	13.67 ± 1.64
Laminin	6.30 ± 0.24	5.87 ± 2.16
FGF2	1.70 ± 1.38	0.74 ± 0.09

Errors represent standard error from at least triplicate experiments.

3.4. Biochemical characterization

A survey of the biochemical components of OFM was undertaken using suitable biochemical assays to confirm the presence of native ECM components in OFM (Tables 1A and B). This targeted important structural proteins, as well as, secondary macromolecules that are associated with the ECM and important during tissue regeneration. In the absence of appropriate purified or recombinant ovine reference standards we assumed that the interspecies reactivity of target proteins would be approximately equal. This is in part justifiable due to the close sequence homology between mammalian structural proteins (data not shown). Total collagen was quantified using a hydroxyproline analysis according to established procedures [28]. Samples were hydrolyzed, then hydroxyproline residues reacted to form a pyrrole chromophore that was quantified using absorbance. As expected, OFM was approximately 80% collagen by dry weight. Herovici's tissue stain is known to specifically differentiate collagens I (red) and III (blue) [29], and demonstrated that collagens I and III were present in ovine forestomach tissue and OFM at a ratio of approximately 3:2 and 9:1, respectively (Fig. 1E and F). This finding was consistent with a collagen analysis using the delayed reducing SDS-PAGE technique of Sykes et al. [21]. This approach made it possible to resolve the constituent α1 (III), α1 (I) and α2 (I) subunits of collagens I and III, and hence determine the relative proportions of

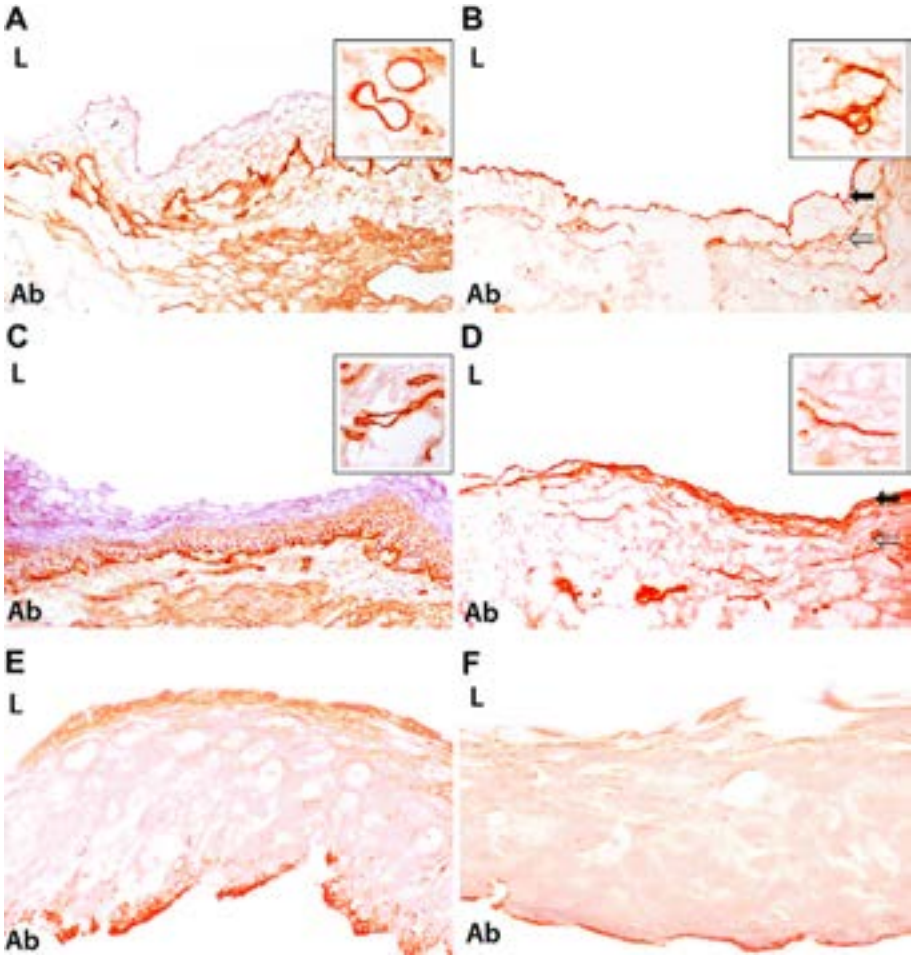

Fig. 2. Representative images of collagen IV (A and B) and laminin (C and D) stained ovine forestomach (A and C) and OFM (B and D). 20× Magnification. Representative images of collagen IV (E) and laminin (F) staining of the lamina epithelias. 40× Magnification. Immunoreactivity appears as red-brown. Location of the basement membrane '←', and dense connective layer '⇐'. Inserts show blood vessel staining. Luminal and abluminal surfaces are indicated with 'L' and 'Ab', respectively.

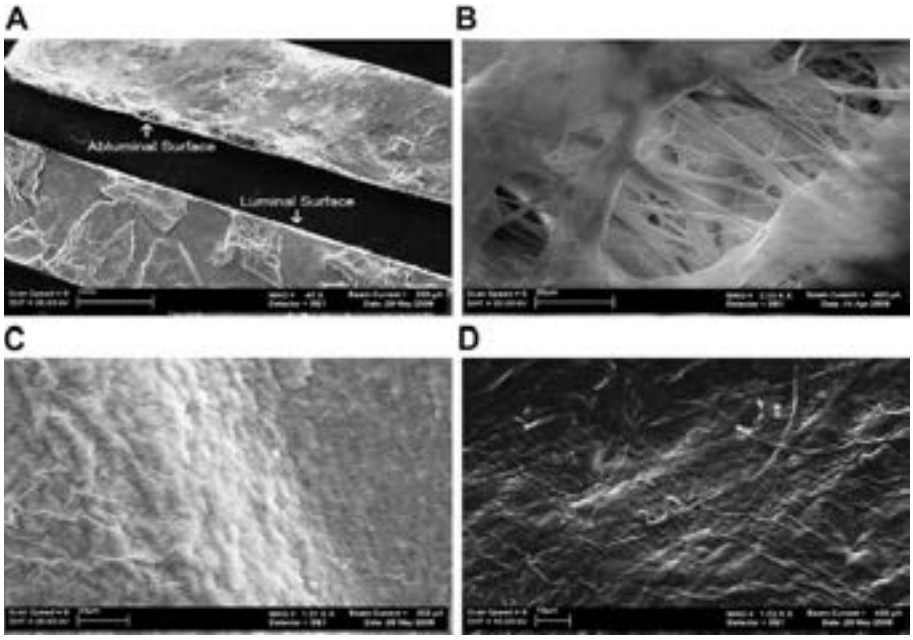

Fig. 3. (A) Low magnification comparison of the luminal and abluminal surfaces of OFM using SEM. (B) The complex collagenous microarchitecture underlying the luminal surface. High magnification of the luminal (C) and abluminal surfaces (D).

collagens I and III (Fig. 4). Due to the relative impurity of the forestomach tissue extract it was necessary to firstly salt precipitate the collagens. SDS-PAGE and subsequent densitometric analysis demonstrated that the collagen I:III ratios were 88% ± 2%:12% ± 2% and 74% ± 3%:26% ± 4% for OFM and forestomach tissue, respectively. Collagens I and III concentrations of OFM and ovine forestomach were further quantified by ELISA. In general, there was good agreement between the three approaches (Herovici staining, SDS-PAGE and ELISA) for the determination of collagens I and III ratios in OFM and ovine forestomach. Collagen IV (9.7 ± 2.1 mg/g) represented only a fraction (approx. 1%) of the total collagen present in OFM. Immunohistochemistry confirmed the presence of collagen IV in OFM and its localization to the junction of the epithelial and endothelial layers (see above).

Elastin is a structural protein characterized by an extensive covalent array arising from cross-linking of the soluble tropoelastin monomers. Given its extensive lysine cross-linking elastin is especially insoluble and therefore challenging to quantify in biological samples. We attempted to quantify elastin using the Fastin™ Elastin Kit by firstly solubilizing tissue in 0.25 M oxalic acid (105 °C, 16 h), according to published procedures [30]. However, the difficulty in fully solubilizing tissues prior to analysis meant that we were unsure that this approach gave truly representative elastin concentrations. As an alternative, we used the mass balance method of Wolinsky [31], whereby samples were subjected to a series of solvent and detergent extractions to isolate the soluble ECM components and yield the insoluble elastin component. Insoluble elastin was calculated by comparing the dry weight of the sample before and after extraction. The elastin concentration of OFM was 41.4 ± 5.0 mg/g. Using this approach it was also possible to determine the lipid content (59.0 ± 5.2 mg/g) of OFM by comparing the mass balance before and after ethanol/diethyl ether extraction.

Total GAGs were quantified using a colorimetric dye-binding assay (Blyscan Sulfated Glycosamine Kit) following papain digestion of powdered tissue samples. OFM had a total GAG concentration of 0.74 ± 0.01 mg/g and a Safranin-O proteoglycan stain demonstrated the diffuse distribution of GAGs throughout the ECM (Fig. 1G and H). Papain-digested samples of OFM were additionally resolved by cellulose acetate GAG gel electrophoresis according to established procedures [32]. GAGs present in OFM samples migrated similarly to a standard sample of HS, but not chondroitin

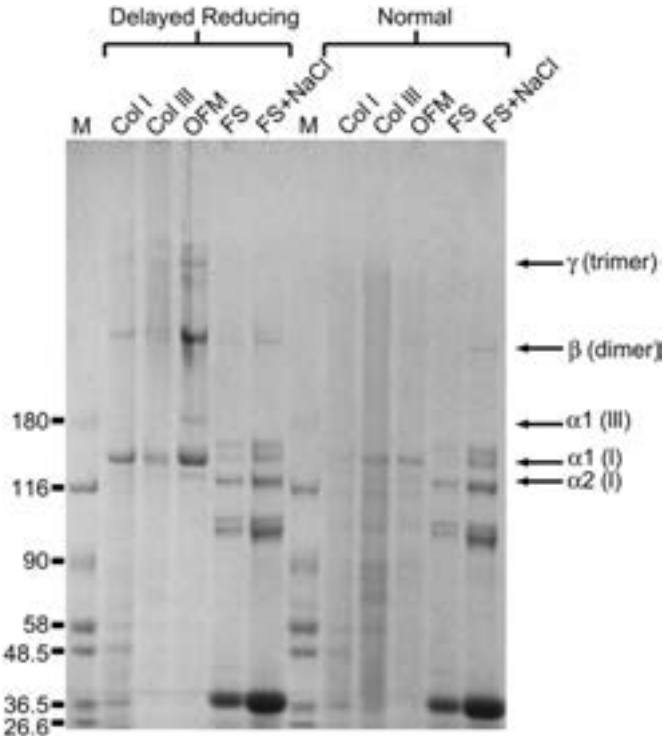

Fig. 4. SDS-PAGE analysis of collagen sin OFM and forestomach tissue. 'M' = molecular weight markers; 'col I' human collagen I standard; 'col III' human collagen III standard; 'FS' = forestomach tissue extract; 'FS + NaCl' = salt precipitated forestomach tissue extract. Samples were run under delayed reducing conditions or under 'normal' reducing conditions.

sulfate B, or HA (data not shown). Densitometric analysis of the Alcian blue stained cellulose acetate gel demonstrated the amount of HS present in OFM was approximately 0.2 mg/g. The presence of HS was further confirmed by quantifying total GAGs, both before (0.74 ± 0.01 mg/g), and after (0.43 ± 0.01 mg/g) a heparan lyase digestion of an OFM extract. This approach assumed disaccharides are unreactive to the Blyscan GAG assay. Based on this analysis, lyase sensitive HS represented approximately 40% of total GAGs present in OFM, or a concentration of 0.31 ± 0.01 mg/g. This finding was in line with the cellulose acetate gel electrophoresis analysis described above. However, HS did not account for the total GAGs as measured in OFM. Therefore, OFM extracts were additionally analyzed by HPLC to establish the presence of chondroitin sulfate, another major GAG that may be expected to be present in OFM. A papain-digested extract of OFM was further digested using chondroitinase ABC to hydrolyze chondroitin to constituent monomers. The chondroitinase digested extract was analyzed by HPLC and demonstrated that none of the expected monomers of chondroitin sulfate were present. This finding implies that if chondroitin sulfate is present in OFM it is at concentrations less than the limit of detection for this method, and therefore significantly less than heparan sulfate. Hyaluronic acid was also quantified in OFM extracts at concentrations of 0.31 ± 0.01 mg/g using ELISA.

OFM and ovine forestomach were analyzed for the minor biochemical components, fibronectin, laminin and FGF2 (Table 1B). In all cases, minor components were quantified from a 4% SDS extract using ELISA. The concentration of fibronectin in OFM was shown to be 13.67 ± 1.64. Additional studies demonstrated that the concentration of fibronectin in SIS was significantly less than OFM, at 5.00 ± 0.05 μg/g. Laminin and FGF2 were both shown to be present in OFM (5.87 ± 2.16 μg/g, and 0.74 ± 0.0.09 μg/g, respectively).

3.5. Cell adhesion and infiltration

To assess any toxic response of mammalian cells to OFM, extracts of the matrix were prepared and applied to a cell monolayer of D551 cells [33]. Matrix was incubated with DMEM for 24 h, then supplemented with 10% FCS and applied directly to a cell monolayer of D551 cells. Cells were incubated in the presence of OFM-conditioned media for 72 h, and the cell density was quantified using a formazan (MTT) dye assay. Cell density in the presence of OFM extract was not reduced relative to untreated control cells. Additionally, there were no morphological differences observed between treated and untreated cells.

Studies were undertaken to determine binding of keratinocyte and fibroblast cells to the surface of OFM. Additionally, given the presence of residual basement membrane components and the anisotropic surfaces of OFM, we sought to understand if there was preferential binding of either cell type to the luminal or abluminal surfaces. Keratinocytes and fibroblasts were seeded onto the surface of OFM and incubated for 3 h, at which time unbound cells were removed by gently agitation of the matrix. OFM tissues were formalin fixed, stained with DAPI and visualized using fluorescence microscopy. Representative images are provided as Fig. 5A–D. Cells present on the surface of the OFM were quantified and expressed as the average number of cells visible per tissue section (Fig. 5E). Keratinocytes and fibroblasts were shown to readily adhere to both the luminal and the abluminal surfaces of OFM. Adherent cells were visible within approximately 30 min of cell seeding (data not shown). There was better adhesion of fibroblasts to both surfaces relative to keratinocytes (Fig. 5E), and fibroblasts preferentially adhered to the abluminal surface. In contrast, keratinocytes preferentially adhered to the luminal surface, relative to the abluminal.

Fibroblasts were additionally seeded onto OFM matrix and incubated for up to 10 days to assess the cellular infiltration of the matrix. Fibroblasts were seeded to the abluminal surface of OFM and can be seen associated with the abluminal surface at early time points (Fig. 5F). By day 3, cells appeared to have migrated through the matrix towards the luminal surface of the matrix (Fig. 5G), such that by days 3–5 the bulk of the cells were associated with the luminal surface. At day 10 (Fig. 5H), cells were distributed throughout the matrix in a dense three dimensional culture.

3.6. In vitro cell differentiation

To observe any stimulatory activity of OFM on mammalian cells, pheochromocytoma cells of the rat adrenal medulla (PC12) were

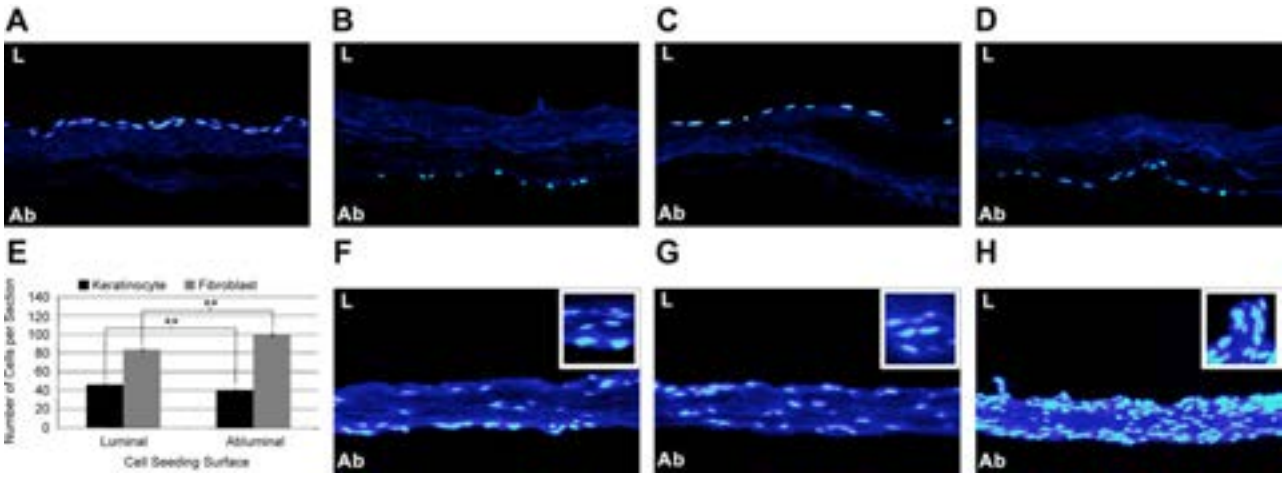

Fig. 5. Cellular adhesion and infiltration of OFM. Representative DAPI stained tissue sections of OFM seeded with either keratinocytes (A and B) or fibroblasts (C and D) to either the luminal (A and C) or abluminal surfaces (B and D). Images B and D have been rotated to maintain the relative orientation of the OFM. 20× Magnification. (E) Quantification of keratinocyte and fibroblast adhesion to either the luminal or abluminal surface of OFM. Error bars represent standard error from at least three independent experiments. **<0.01 by unpaired *T*-test. DAPI stained OFM infiltrated with human fibroblast cells after 0.5 (F), 5 (G) and 10 (H) days. Cells were seeded to the abluminal surface and images have been rotated to maintain the relative orientation of the OFM. 20× Magnification, with 40× magnification inserts. Luminal and abluminal surfaces are indicated with 'L' and 'Ab', respectively.

exposed to OFM extracts and cellular differentiation quantified according to established procedures [34]. On exposure to an SDS extract of OFM, PC12 cells differentiated, as evidenced by the outgrowth of neuronal processes. For example, the number of processes per cell increased approximately 25-fold relative to untreated cells following exposure to the OFM extract at 5.6 mg/mL (Figs. 6 and 7A). The stimulatory activity of the OFM extract was dose dependent, with higher OFM protein concentrations eliciting a more dramatic response.

Findings from an SDS extract of OFM were extended to understand the stimulatory effect of OFM under more physiologically relevant conditions. Thus, a powder of OFM was prepared and incubated at concentrations of 20, 50 and 100 mg/mL in DMEM at 37 °C, overnight. Media was filter sterilized and transferred to PC12 cells. Cell differentiation after 48 h was quantified as described above. Cells treated with an extract prepared from OFM powder at 100 mg/mL increased cell differentiation approximately 20-fold relative to untreated cells. Media extracts stimulated cell differentiation in a dose-dependent manner, as shown in Fig. 7B.

3.7. *In vitro bioactivity of fibroblast growth factor basic*

In order to test the functional state of the FGF2 present in OFM, and to understand its role in the observed cell differentiation, PC12 cells were incubated with an OFM extract that had previously been neutralized with an anti-FGF2 antibody. In this way, the anti-FGF2 antibody would bind directly to FGF2 present in the extract and inhibit FGF2-mediated cell differentiation. The FGF2 concentration (856 ng/mL) of an SDS extract described above was quantified using ELISA, according to established procedures. The SDS extract (total protein concentration 14 mg/mL) was incubated with anti-human FGF2 diluted 1:50, 1:100 and 1:200 for 30 min at 37 °C. The 'neutralized' extract was transferred to a culture of PC12 cells to give a final protein concentration of 1.4 mg/mL. Cell differentiation was quantified as described above. As demonstrated previously, incubation of the SDS extract (total protein concentration 1.4 mg/mL) with PC12 cells increased cell differentiation approximately 7-fold relative to untreated cells (Fig. 7C). Interestingly, the stimulatory effect of the OFM extract (1.4 mg/mL) was not as great as recFGF2, even though the OFM extract contained approximately 50 ng/mL FGF2, as determined previously by ELISA. In the presence of anti-FGF2 antibody (1:500 dilution) the stimulatory effect of the OFM extract was partially blocked. The inhibitory effect of the antibody was dose-dependent, such that an anti-FGF2 antibody concentration of 1:2000 did not inhibit the observed stimulatory effect. OFM components responsible for the stimulatory effect in PC12 cells could also be extracted from OFM using DMEM, as described above. The stimulatory effect of DMEM extracts could also be partially inhibited using an anti-FGF2 antibody (data not shown). These experiments demonstrated that the stimulatory effect of the OFM extract was dependent in part on the growth factor FGF2, and that FGF2 isolated from OFM was bioactive.

4. Discussion

Advances in the field of biomaterials have seen many collagen-based materials developed for current and future clinical applications. Broadly these technologies either make use of reconstituted collagen or collagen purified from tissues as an intact ECM. Reconstituted collagens have found a broad range of applications both in laboratory and clinical settings. However, it is becoming more apparent that these simplistic biomimetics of the ECM lack critical components, both structural and functional, to truly recapitulate native ECM. For example, cell migration is known to be compromised on reconstituted collagen matrices as evidenced by a decrease in the expression of matrix metalloproteases that play a critical role in cell migration [35]. The pioneering work of Badylak and co-workers on the development of intact and native ECM biomaterials, demonstrated the biochemical and in vivo benefits of native ECMs, over reconstituted collagen products [11]. This approach recognizes the important role of the ECM during tissue regeneration and harnesses the natural complexity encoded in native intact ECM biomaterials for tissue regeneration.

Rather than attempt to regenerate an ECM mimetic *de novo* from a reconstituted collagen source, we have developed an ECM biomaterial from ovine tissue that retains the biochemistry and structural properties of native ECM. Numerous methods have been published describing the decellularization of tissues as part of tissue reprocessing (e.g. bone allografts and heart valves) and for the production of ECM- and collagen-based medical devices. Processing methods typically use chemical and/or enzymatic methods to decellularize the tissue, leaving an intact structural framework of connective proteins. As well as decellularizing the tissue, harsh chemical processing methods can often significantly denature the structural proteins. Loss of performance characteristics (e.g. strength and elasticity) as a result of matrix denaturation can be overcome by chemical cross-linking but this in itself can impart unwanted biological properties as a result of these non-native structural features. For example, chemically cross-linked ECM biomaterials are known to invoke a chronic inflammatory response resulting in scar tissue formation [36]. Processing methods are additionally known to reduce the availability of important ECM-bound macromolecules that often impart important biological function to the ECM [13]. Retention of these

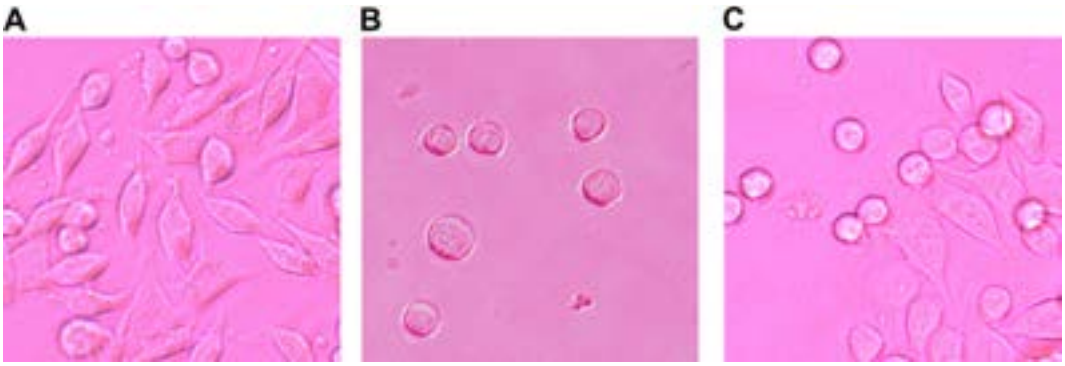

Fig. 6. PC12 cells treated with (A) 50 ng/mL recFGF2; (B) untreated PC12 cells and (C) treated with SDS extract of OFM at 5.6 mg/mL protein concentration. 40× Magnification. (D) Quantification of neuronal differentiation of PC12 cells in the presence of OFM extract. Concentrations indicated are the final protein concentration of OFM extract in culture. Error bars represent standard error from three independent experiments.

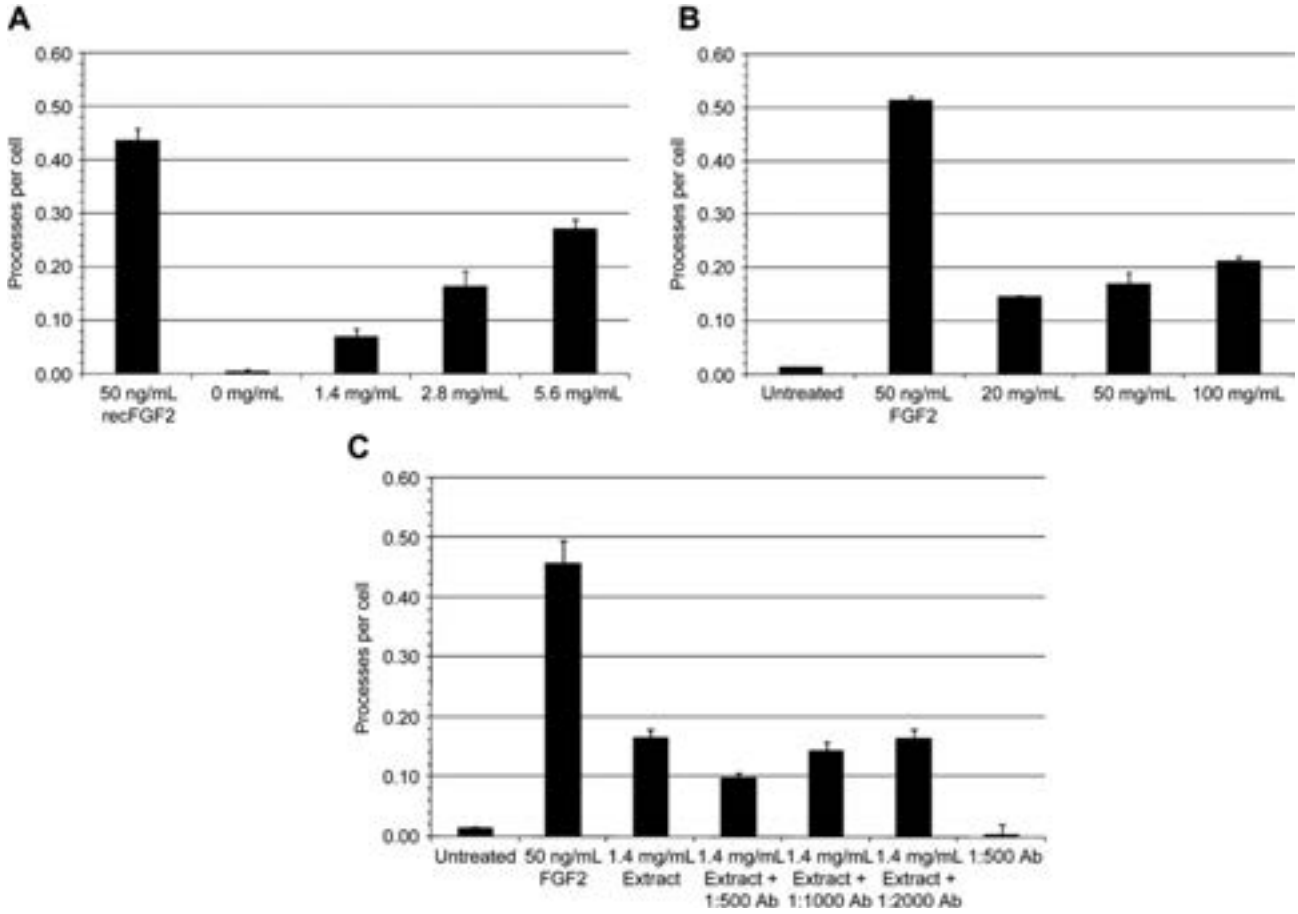

Fig. 7. (A) Differentiation of PC12 cells in the presence of OFM-extracted media. OFM powder was extracted with DMEM at the indicated concentrations. (B) Blocking the stimulatory effect of OFM using anti-FGF2 antibody. Antibody (Ab) dilutions in culture are indicated. Error bars represent standard error from triplicate experiments.

structural and functional features of the ECM biomaterial must be tempered by the need for safety of the end product. Processing methods must address pathogenic and immunogenic risks associated with allogenic and xenogenic implantable material. Therefore, it is important to identify processing methods and raw materials that can reduce disease transmission and immunogenic risks, while retaining the structural integrity and biology of native ECM.

We have developed an osmosis-based method of tissue decellularization, termed STOF. In its current embodiment, the STOF process has been applied to the decellularization of ovine forestomach. However, the STOF process could be applied to a range of tissue or organ types (e.g. arteries, bladders, pericardia or amnion). We found that the STOF process significantly improved the separation of tissue layers and was also amenable to tissue decellularization at reduced temperatures (e.g. 4 °C, data not shown), as penetration of detergents into the tissues was not reliant on simple diffusion. The OFM produced using the STOF process was effectively decellularized (Fig. 1D), as evidenced by the relatively low concentrations of DNA. To understand how these low levels of nucleic acids may affect the immunogenicity of OFM, we quantified DNA in the well established commercial product, SIS. SIS has previously been shown to contain DNA fragments [55], and in our hands both OFM and SIS had equivalent concentrations of DNA (Table 1). The inflammatory response to SIS is well understood and proceeds via the pro-inflammatory pathway characterized by Th2 lymphocyte and M2 macrophage phenotypes, indicative of normal constructive remodeling [5]. Given that the levels of decellularization of OFM and SIS are equivalent, as judged by DNA concentrations, we would expect OFM to elicit a similar inflammatory response. Indeed, in vivo studies to date have confirmed that the inflammatory response to OFM is more consistent with constructive remodeling than chronic inflammation (unpublished data).

The role of functional biomaterials in tissue regeneration is 2-fold. Firstly, they must provide the microarchitecture required for cellular infill and the mechanical support to maintain tissue integrity during the regeneration process. Secondly, necessary co-factors must be present within the biomaterial to guide tissue regeneration by orchestrating cell–cell and cell–ECM signaling. We have demonstrated that OFM retains many structural features of native ECM, features that are known to impart beneficial properties during tissue regeneration. For example, an examination of OFM by histology and SEM revealed an especially dense continuous layer of collagenous ECM that retained organized open pores extending through the matrix. OFM was shown to be anisotropic, with a dense luminal surface that contrasted the more typical open matrix structure of the abluminal surface. The luminal surface contained residual basement membrane components, including collagen IV and laminin and was characterized by a relatively smooth appearance, as seen by SEM [26]. Collagen IV forms the basis of the collagenous matrix that defines the basement membrane and participates in cell adhesion, especially via laminin which in turn binds heparan sulfate and integrin receptors. It was thought that the presence of residual basement membrane components would direct keratinocyte adhesion and migration along the luminal surface of OFM, eventually leading to cellular

infill of the matrix [37]. Our own studies demonstrated that keratinocytes preferentially bound to the luminal surface, most likely via laminin present in the remnants of the basement membrane. We do not think that the basement membrane remained intact following the STOF process. This was evidenced by collagen IV and laminin immunoreactivity on the abluminal surface of the lamina epithelias, consistent with fracturing of the basement membrane during delamination of the lamina epithelias and propria submucosal layers. Collagen IV and laminin were also quantified in the lamina epithelias using ELISA (658 ± 44 μg/g and 17.3 ± 1.1 μg/g). Basement membrane components were also evident in the remnants of vascular channels within OFM and would therefore be available during repopulation of the channels by endogenous endothelial cells. A continuous basement membrane has previously been reported for the porcine urinary bladder matrix, but is absent in SIS [26]. A consequence of the forestomachs normal function in storage and fermentation is the relative thickness and elasticity encoded in the collagenous microarchitecture of OFM. For example, OFM is significantly thicker (300 μm) than intestinal submucosa derived SIS (100 μm, [38]). These structural features impart excellent biophysical characteristics to the OFM which make it an ideal biomaterial for load-bearing implant applications (e.g. hernioplasty or breast reconstruction) where the biomaterial must function in a supportive role during tissue regeneration.

As well as the structural proteins (collagens and elastin), OFM also retained many biologically significant macromolecules which are important in tissue regeneration and proper functioning of the ECM. These included fibronectin, laminin, HS, HA and FGF2. Fibronectin plays a central role in ECM–cell interactions via binding interactions with a variety of cell-surface and ECM-bound molecules, including collagens, integrins and GAGs [39]. Via these interactions, fibronectin promotes the attachment and migration of a number of cell types. Once excreted from cells, fibronectin self assembles and matures to form a fibronectin matrix which complements the structural features of the collagen matrix by providing elasticity and recoil. The concentrations of fibronectin were especially high in OFM relative to SIS. Given the important role that fibronectin plays as an adhesive protein during wound healing, these findings suggest OFM may have advantageous regenerative properties relative to SIS. HS is an important ECM-bound GAG that serves as a co-factor to FGF2 bioactivity by binding directly to FGF2 receptors in the presence of FGF2, thus stabilizing the FGF2-receptor complex [40]. HS also binds free FGF2, stabilizing the growth factor and prolonging its circulating half-life [41]. HS was shown to make up only a portion of the total measured GAGs present in OFM, while chondroitin sulfate was not detectable. This suggests that other GAGs are likely to be present in OFM, and further studies will be necessary to identify and quantify these additional GAG components. OFM extracts were shown to stimulate cell differentiation, and the stimulatory effect was shown to be due in part to the presence of bioactive FGF2. FGF2 is a multifunctional growth factor that plays an important role in tissue regeneration, including the promotion of endothelial cell differentiation during angiogenesis, and cell differentiation and migration of a number of cell types. The fact that ovine FGF2 extracted from OFM is able to signal differentiation in PC12 cells is extremely encouraging and suggests that OFM FGF2 (and/or other stimulatory growth factors) present in OFM may be available to stimulate positive cellular responses in human tissue regeneration. In our current studies OFM-extracted FGF2 was not as potent as human recFGF2. The differences in the observed response may be attributed to a host of factors but most obviously a differential susceptibility of mouse PC12 cells to human FGF2 compared with ovine FGF2. It was not possible, even with high concentrations of anti-FGF2 antibody, to completely inhibit the stimulatory effect of the OFM extracts. This suggests that there may be additional components in the OFM extract (e.g. growth factors or GAGs) that also contribute to the observed stimulatory effect. Further studies are underway to understand the contribution of these additional components to the observed bioactivity of OFM. The presence of important ECM co-factors, as well as, the demonstrated bioactivity of OFM in culture supports the functional properties of OFM. The functional properties of OFM, as well as its structural features, suggest this biomaterial is ideally suited to wound healing and soft tissue regeneration.

Clinical applications for native ECM in wound healing and tissue regeneration span a range of size, format and strength requirements. In the search for alternate source tissues from which to prepare ECMs we identified the ovine forestomach. The forestomach is substantially larger than the glandular stomach and has gross anatomical and histological features that are quite distinct also. For example, the forestomach does not contain a glandular mucosa, but is instead comprised of a non-glandular keratinized stratified squamous epithelium, which appears in many respects analogous to the structure of human skin. One feature of the forestomach that was retained in OFM was an especially dense layer of connective tissue present in the propria submucosa (Fig. 1A and B). This layer has previously been described in the forestomachs of several species, and referred to as a ‘condensed fibrous layer’ [42]. As a consequence of its primary role in storage and fermentation, the fully distended forestomach has a volume of approximately 15 L, making it one of the largest available organs for the production of intact ECMs. In this way, it is possible to produce large format single sheets of OFM (approx. 40 × 40 cm) which would be especially suitable for application to large tissue deficits, for example pressure ulcers and burns.

Native and reconstituted animal collagens are well tolerated in humans due to the close sequence homology between mammalian collagens. As such, the biocompatibility of collagens from a variety of mammalian sources is well established in a number of clinical applications. Ovine collagens have traditionally been used in the manufacture of surgical suture (catgut) sourced from the fibrous submucosal layer of ovine intestines, analogous to porcine SIS. Published reports have also described the use of ovine pericardium as a dural substitute [43], ovine dermal collagen for chest and abdominal wall reconstructions in animal models [44], ovine derived vascular grafts [45] and decellularized ovine heart valves [46]. In vivo characterization of ovine collagens, as well as, the established clinical use of ovine collagen in the form of catgut, demonstrates that the risk of deleterious inflammatory response to OFM would be low. Indeed, in vivo studies by our group have confirmed the biocompatibility of OFM, and its ability to undergo remodeling as part of normal tissue regeneration (unpublished data).

It is difficult to quantitatively ascertain if the uptake of various animal and/or human-derived collagen biomaterials is reduced due to cultural and/or religious sensitivities. Only a few studies describing the cultural acceptability of animal- and cadaver-based surgical implants have been published [47]. Collectivity these reports reinforce the right of the patient to ‘manifest his religion or belief in worship, teaching, practice and observance’ [48] through informed consent. Given the preference of several groups to not receive porcine, bovine and cadaveric implants, it seems sensible from a clinical perspective to offer suitable alternatives. As such, ovine tissues are an obvious source of culturally acceptable collagens for clinical and cosmetic applications. An additional attractive feature of ovine collagens is the low disease transmission risk these present relative to human, bovine or porcine-derived collagens. For example, relatively few ovine viruses pose serious zoonotic risk, and of the ovine viruses present in New Zealand sheep, only the

parapox virus causing Orf disease and parainfluenza type 3 virus have been reported to cause disease in humans [49]. Additionally, there have been concerns raised over the potential transmission of prion disease from animal- and human-derived collagens [50]. While human-to-human, and bovine-to-human prion transmission have been demonstrated both clinically and experimentally [51,52], epidemiological evidence does not support the transmission of ovine prions (scrapie) to humans [53]. In fact, current evidence supports the existence of a species barrier that specifically protects humans from ovine prions [54]. The existence of a species barrier to prion transmission, as well as New Zealand's accepted 'prion-free' status [53], imparts added safety assurances to OFM, relative to alternate ECM-based biomaterials sourced from other species and other countries.

5. Conclusion

We have developed an osmosis-based method of tissue decellularization and using this approach we have generated a new biomaterial comprising ovine forestomach ECM. The OFM biomaterial presented here demonstrated the structural features of native ECM, as well as, a diverse biochemical composition consistent with native ECM. In vitro, OFM was non-cytotoxic to mammalian cells, able to support cell growth and stimulated cell differentiation. The large format and inherent strength of OFM suggest it will be compatible with a number of clinical applications, both in wound healing and tissue regeneration. Being of ovine origin, it is expected that the clinical application of OFM will not be limited by religious or cultural considerations.

Acknowledgements

We would like to acknowledge the Foundation for Research Science and Technology (New Zealand) MSMA0701 and New Zealand Trade and Enterprise for funding this project. The authors would like to thank Nancy Yopp and Professor Gregory Schultz for critical reading of this manuscript. SEM was conducted with the assistance of Scott Morgan and James Xia (IRL, New Zealand).

Author disclosure statement

BRW is a shareholder of Mesynthes Limited.

Appendix

Figures with essential color discrimination. Figs. 1, 2, 5 and 6 in this article are difficult to interpret in black and white. The full color images can be found in the online version, at doi:10.1016/j.biomaterials.2010.02.025.

References

[1] Badylak SF. The extracellular matrix as a biologic scaffold material. Biomaterials 2007;28:3587–93.
[2] Gilbert TW, Stewart-Akers AM, Simmons-Byrd A, Badylak SF. Degradation and remodeling of small intestinal submucosa in canine Achilles tendon repair. J Bone Joint Surg Am 2007;89:621–30.
[3] Lantz GC, Badylak SF, Hiles MC, Coffey AC, Geddes LA, Kokini K, et al. Small intestinal submucosa as a vascular graft: a review. J Invest Surg 1993;6:297–310.
[4] Li F, Li W, Johnson S, Ingram D, Yoder M, Badylak S. Low-molecular-weight peptides derived from extracellular matrix as chemoattractants for primary endothelial cells. Endothelium 2004;11:199–206.
[5] Badylak SF, Gilbert TW. Immune response to biologic scaffold materials. Semin Immunol 2008;20:109–16.
[6] Silverman RP, Li EN, Holton 3rd LH, Sawan KT, Goldberg NH. Ventral hernia repair using allogenic acellular dermal matrix in a swine model. Hernia 2004;8:336–42.
[7] Stump A, Holton 3rd LH, Connor J, Harper JR, Slezak S, Silverman RP. The use of acellular dermal matrix to prevent capsule formation around implants in a primate model. Plast Reconstr Surg 2009;124:82–91.
[8] Buinewicz B, Rosen B. Acellular cadaveric dermis (AlloDerm): a new alternative for abdominal hernia repair. Ann Plast Surg 2004;52:188–94.
[9] Sarikaya A, Record R, Wu CC, Tullius B, Badylak S, Ladisch M. Antimicrobial activity associated with extracellular matrices. Tissue Eng 2002;8:63–71.
[10] Hodde J, Hiles M. Constructive soft tissue remodelling with a biologic extracellular matrix graft: overview and review of the clinical literature. Acta Chir Belg 2007;107:641–7.
[11] Badylak SF, Freytes DO, Gilbert TW. Extracellular matrix as a biological scaffold material: structure and function. Acta Biomater 2009;5:1–13.
[12] Grauss RW, Hazekamp MG, Oppenhuizen F, van Munsteren CJ, Gittenberger-de Groot AC, DeRuiter MC. Histological evaluation of decellularised porcine aortic valves: matrix changes due to different decellularisation methods. Eur J Cardiothorac Surg 2005;27:566–71.
[13] Gilbert TW, Sellaro TL, Badylak SF. Decellularization of tissues and organs. Biomaterials 2006;27:3675–83.
[14] Ward BR, Johnson KD, May BCH. Tissue scaffolds derived from forestomach extracellular matrix. US Patent No. 12/512,835; 2009.
[15] Badylak SF, Lantz GC, Coffey A, Geddes LA. Small intestinal submucosa as a large diameter vascular graft in the dog. J Surg Res 1989;47:74–80.
[16] Bancroft JD, Stevens A. Theory and practice of histological techniques. 3rd ed. Edinburgh, New York: Churchill Livingstone; 1990.
[17] Cook HC. Manual of histological demonstration techniques. London: Butterworths; 1974.
[18] An YH, Martin KL. Handbook of histology methods for bone and cartilage. Totowa, NJ: Humana Press; 2003.
[19] Reddy GK, Enwemeka CS. A simplified method for the analysis of hydroxyproline in biological tissues. Clin Biochem 1996;29:225–9.
[20] Harding JJ, Wesley JM. The purification and amino acid composition of human uterus collagens, rheumatoid-arthritis-nodule collagen and ox tendon collagen. Biochem J 1968;106:749–57.
[21] Sykes B, Puddle B, Francis M, Smith R. The estimation of two collagens from human dermis by interrupted gel electrophoresis. Biochem Biophys Res Commun 1976;72:1472–80.
[22] May BC, Fafarman AT, Hong SB, Rogers M, Deady LW, Prusiner SB, et al. Potent inhibition of scrapie prion replication in cultured cells by bis-acridines. Proc Natl Acad Sci U S A 2003;100:3416–21.
[23] Jacobi U, Kaiser M, Toll R, Mangelsdorf S, Audring H, Otberg N, et al. Porcine ear skin: an in vitro model for human skin. Skin Res Technol 2007;13:19–24.
[24] Seddon SV, Walker DM, Williams D, Williams ED. The clonal organization of the squamous epithelium of the tongue. Cell Prolif 1992;25:115–24.
[25] Gilbert TW, Freund JM, Badylak SF. Quantification of DNA in biologic scaffold materials. J Surg Res; 2008.
[26] Brown BN, Barnes CA, Kasick RT, Michel R, Gilbert TW, Beer-Stolz D, et al. Surface characterization of extracellular matrix scaffolds. Biomaterials; 2009.
[27] Baer E, Cassidy JJ, Hiltner A. Hierarchical structure of collagen composite systems: lessons from biology. Pure Appl Chem 1991;63:961–73.
[28] Edwards CA, O'Brien Jr WD. Modified assay for determination of hydroxyproline in a tissue hydrolyzate. Clin Chim Acta 1980;104:161–7.
[29] Rawlins JM, Lam WL, Karoo RO, Naylor IL, Sharpe DT. Quantifying collagen type in mature burn scars: a novel approach using histology and digital image analysis. J Burn Care Res 2006;27:60–5.
[30] Wilshaw SP, Kearney JN, Fisher J, Ingham E. Production of an acellular amniotic membrane matrix for use in tissue engineering. Tissue Eng 2006;12:2117–29.
[31] Wolinsky H. Response of the rat aortic media to hypertension. Morphological and chemical studies. Circ Res 1970;26:507–22.
[32] Stanley RA, Lee SP, Roberton AM. Heterogeneity in gastrointestinal mucins. Biochim Biophys Acta 1983;760:262–9.
[33] Mirsadraee S, Wilcox HE, Korossis SA, Kearney JN, Watterson KG, Fisher J, et al. Development and characterization of an acellular human pericardial matrix for tissue engineering. Tissue Eng 2006;12:763–73.
[34] Das KP, Freudenrich TM, Mundy WR. Assessment of PC12 cell differentiation and neurite growth: a comparison of morphological and neurochemical measures. Neurotoxicol Teratol 2004;26:397–406.
[35] Sudbeck BD, Parks WC, Welgus HG, Pentland AP. Collagen-stimulated induction of keratinocyte collagenase is mediated via tyrosine kinase and protein kinase C activities. J Biol Chem 1994;269:30022–9.
[36] Badylak SF, Valentin JE, Ravindra AK, McCabe GP, Stewart-Akers AM. Macrophage phenotype as a determinant of biologic scaffold remodeling. Tissue Eng Part A 2008;14:1835–42.
[37] Brown B, Lindberg K, Reing J, Stolz DB, Badylak SF. The basement membrane component of biologic scaffolds derived from extracellular matrix. Tissue Eng 2006;12:519–26.
[38] McPherson TB, Badylak SF. Characterization of fibronectin derived from porcine small intestinal submucosa. Tissue Eng 1998;4:75–83.
[39] Wierzbicka-Patynowski I, Schwarzbauer JE. The ins and outs of fibronectin matrix assembly. J Cell Sci 2003;116:3269–76.
[40] Friesel RE, Maciag T. Molecular mechanisms of angiogenesis: fibroblast growth factor signal transduction. FASEB J 1995;9:919–25.
[41] Gospodarowicz D, Cheng J. Heparin protects basic and acidic FGF from inactivation. J Cell Physiol 1986;128:475–84.

[42] Banks WJ. Applied veterinary histology. 3rd ed. St. Louis: Mosby-Year Book; 1993.
[43] Parizek J, Mericka P, Husek Z, Suba P, Spacek J, Nemecek S, et al. Detailed evaluation of 2959 allogeneic and xenogeneic dense connective tissue grafts (fascia lata, pericardium, and dura mater) used in the course of 20 years for duraplasty in neurosurgery. Acta Neurochir (Wien) 1997;139:827–38.
[44] Rudolphy VJ, Tukkie R, Klopper PJ. Chest wall reconstruction with degradable processed sheep dermal collagen in dogs. Ann Thorac Surg 1991;52:821–5.
[45] Koch G, Gutschi S, Pascher O, Fruhwirth H, Glanzer H. Analysis of 274 Omniflow Vascular Prostheses implanted over an eight-year period. Aust N Z J Surg 1997;67:637–9.
[46] Steinhoff G, Stock U, Karim N, Mertsching H, Timke A, Meliss RR, et al. Tissue engineering of pulmonary heart valves on allogenic acellular matrix conduits: in vivo restoration of valve tissue. Circulation 2000;102:III50–55.
[47] Easterbrook C, Maddern G. Porcine and bovine surgical products: Jewish, Muslim, and Hindu perspectives. Arch Surg 2008;143:366–70. Discussion 370.
[48] United Nations General Assembly. The universal declaration of human rights. New York: King Typographic Service Corp.; 1949.
[49] Krauss H. Zoonoses: infectious diseases transmissible from animals to humans. 3rd ed. Washington, DC: ASM Press; 2003.
[50] Carruthers J, Carruthers A. Mad cows, prions, and wrinkles. Arch Dermatol 2002;138:667–70.
[51] Scott MR, Peretz D, Nguyen HO, Dearmond SJ, Prusiner SB. Transmission barriers for bovine, ovine, and human prions in transgenic mice. J Virol 2005;79:5259–71.
[52] Will RG. Acquired prion disease: iatrogenic CJD, variant CJD, kuru. Br Med Bull 2003;66:255–65.
[53] Will RG. Epidemiology of Creutzfeldt-Jakob disease. Br Med Bull 1993;49:960–70.
[54] Prusiner SB, Scott M, Foster D, Pan KM, Groth D, Mirenda C, et al. Transgenetic studies implicate interactions between homologous PrP isoforms in scrapie prion replication. Cell 1990;63:673–86.
[55] Zheng MH, Chen J, Kirilak Y, Willers C, Xu J, Wood D. Porcine small intestine submucosa (SIS) is not an acellular collagenous matrix and contains porcine DNA: possible implications in human implantation. J Biomed Mater Res B Appl Biomater 2005;73:61–7.